






## Research Article

# Investigation of Mechanical Behavior and Microstructure Analysis of AA7075/SiC/B<sub>4</sub>C-Based Aluminium Hybrid Composites

HassabAlla M. A. Mahmoud,<sup>1</sup> P. Satishkumar ,<sup>2</sup> Yenda Srinivasa Rao ,<sup>3</sup> Rohinikumar Chebolu,<sup>4</sup> Rey Y. Capangpangan ,<sup>5</sup> Arnold C. Alguno,<sup>6</sup> Mahesh Gopal ,<sup>7</sup> A. Firos ,<sup>8</sup> and Murthi C. Saravana <sup>9</sup>

<sup>1</sup>Department of Physics, Faculty of Sciences and Arts, Dhahran Al Janoub, King Khalid University, Abha, Saudi Arabia

<sup>2</sup>Anna University, Chennai, Tamilnadu, India

<sup>3</sup>Mechanical Engineering, Swamy Vivekananda Engineering College, Bobbili, Andhra Pradesh, India

<sup>4</sup>Mechanical Engineering AUCE(A), Andhra University, Visakhapatnam, Andhra Pradesh, India

<sup>5</sup>Department of Physical Science and Mathematics, College of Science and Environment, Mindanao State University, Naawan, Misamis Oriental, Marawi, Philippines

<sup>6</sup>Department of Physics, Mindanao State University, Lligan Institute of Technology, Lligan City, Philippines

<sup>7</sup>Mechanical Engineering, College of Engineering and Technology, Wollega University, Post Box No. 395, Nekemte, Ethiopia

<sup>8</sup>Department of Computer Science and Engineering, Rajiv Gandhi University, Doimukh, Arunachal Pradesh, India

<sup>9</sup>Mechanical Engineering, United Institute of Technology, Coimbatore, Tamil Nadu, India

Correspondence should be addressed to Mahesh Gopal; [doctorgmahesh@gmail.com](mailto:doctorgmahesh@gmail.com)

Received 4 June 2022; Accepted 5 July 2022; Published 22 July 2022

Academic Editor: Pudhupalayam Muthukutti Gopal

Copyright © 2022 HassabAlla M. A. Mahmoud et al. This is an open access article distributed under the Creative Commons Attribution License, which permits unrestricted use, distribution, and reproduction in any medium, provided the original work is properly cited.

The microstructure and mechanical properties of an MMC based on AA 7075 and strengthened through silicon carbide (SiC) as well as boron carbide (B<sub>4</sub>C) elements were studied. The (SiC + B<sub>4</sub>C) combination was used in various weight percentages of 4, 8, 12, and 16% to create the hybrid composites utilizing the traditional stir casting procedure. XRD and SEM measurements were used to investigate the dispersion of the reinforced particles. For example, microhardness, impact strength, and ultimate tensile strength were measured on hybrid composites at room temperature. The density and porosity of the materials were also studied. The researchers found that increasing the weight percentage of the (SiC + B<sub>4</sub>C) mixture resulted in a small drop in % elongation. However, hybrid composites comprising 16% (SiC + B<sub>4</sub>C) weight reduction showed some decrease in hardness and tensile strength. Equated to unreinforced alloys, the hardness and tensile strength of hybrid composites rise by 8% and 21%, respectively. Reinforcement also resulted in a decrease in impact strength and density, as well as an increase in porosity.

## 1. Introduction

Metal matrix composites (AMCs) made of aluminium have gained popularity in recent decades because of their amazing qualities such less weight, higher strength, modulus of elasticity, exceptional restraining, and good wear resistance. When the number of reinforced particles in a matrix composition grows, ductility often suffers [1]. In transportation

and structural applications, where high-stress resistance is critical, 6082 T6 tweaked AA provides good mechanical qualities and high strength [2]. Aluminium composites have undergone a great deal of development in the last few decades to improve their qualities [3].

Hybrid aluminium AMCs are the next generation of AMCs, and they have the ability to fulfill the growing demands of high-tech applications in the future [4]. Additionally,

researchers have experimented with creating hybrid metal matrix composites by combining two or more reinforcing materials, in an effort to get better mechanical qualities, such as increased dimensional stability and improved heat and corrosion resistance for the final invention [5]. A number of researchers have explored the mechanical properties of a range of hybrid composites. As per the proportion of strengthening in the metal matrix increases, tensile strength, stiffness, and porosity all improve. However, when the proportion of reinforcement rises, the composite's impact energy and density both fall significantly. Ultrasonic cavitation solidification was used in [6] to create a hybrid composite utilizing AA6061 as a base metal and (SiC + B<sub>4</sub>C) as reinforcement. They found that the porosity boosted the hardness and tensile strength of the alloy. When [7] used a traditional stir casting method to create a hybrid composite, they used an aluminium alloy containing boron carbide (B<sub>4</sub>C) and graphite reinforcing particles (Gr). For better strength, hardness, and wear resistance, researchers added B<sub>4</sub>C to the matrix, but the material became more brittle as a result. Alumina nanoparticles (Al<sub>2</sub>O<sub>3</sub>) were created via powder metallurgy, and the strengthening mechanism was discovered to be the most important strength mechanism [8, 9]. The solidification of a substance is linked to the program of dislocations inside that material. Strengthening mechanisms must be introduced to limit dislocation movement and thus boost the material's strength in order to improve material attributes like yield strength. Researchers evaluated the wear as well as the mechanical characteristics of reinforcement combinations on the surface of composites for wear [10]. An increase in microhardness is attributed to the occurrence of silicon carbide and alumina particles in hybrid composites made of Al, SiC, and Gr. SiC and Al<sub>2</sub>O<sub>3</sub> reinforcement added to aluminium hybrid composites boosted tensile strength and hardness while decreasing the elongation percentage, according to a study by Davis et al. [11]. It was found that the ultimate tensile and hardness of hybrid composites made with boron carbide particles and calcium carbide with the main alloy of AA 6063 were improved, while the impact strength was somewhat reduced. A two-step stir casting procedure was used to create a dual-reinforced particle AA composite in [12]. LM-13 AA was used in the experiments. Silicon carbide and zircon sand (ZrSiO<sub>4</sub>) particles were used in the study. The composites outperform the unreinforced alloy in terms of wear resistance, according to the authors.

It is stated in the literature that several researchers have evaluated the mechanical and structural properties of composite materials using SiC, Gr, Ca<sub>2</sub>O<sub>3</sub>, ZrSiO<sub>4</sub>, TiC, and Al<sub>2</sub>O<sub>3</sub>. There has been no study done on AA6082 to make hybrid composites employing (SiC + B<sub>4</sub>C) as reinforcement. Aluminum and silicon carbide (SiC) particles are chemically compatible and create strong bonds in the matrix [13]. There are a number of advantages to using SiC as a reinforcement in AMCs because of its outstanding workability, easy machining, and inexpensive cost. B<sub>4</sub>C must be added to aluminium composites in order to increase their mechanical qualities. B<sub>4</sub>C is a great reinforcement material because of its high rigidity and hardness, as well as its low density. Because of B<sub>4</sub>C and aluminum's similar densities, the settling

problem is reduced while solidifying a molten matrix due to its low density [14]. An initial investigation of the (SiC + B<sub>4</sub>C)-reinforced AA6082 hybrid composites' microstructure and mechanical characteristics was carried out. Many different techniques, including liquid state production, stir casting, intrusion, and squeeze casting, can be utilized to make composites. The stir casting process is the most commonly used technique for composite manufacturing because it can generate complex shapes at a low cost. Using a graphite crucible to melt a molten matrix metal requires 10–15 minutes of vigorous stirring in order to produce a homogeneous composite [15]. When it comes to liquid state manufacturing, stir casting is the most easy and cost-effective process. Another benefit of the stir casting technology is its capacity to produce composites with a volume proportion of up to 30%. [16–18]. The swirling motion of the particles in the stir casting process enhances the chemical interactions between the matrix and reinforcing particles [19]. Experimental data on microhardness, impact strength, elongation percentage, and tensile strength of stir-cast hybrid metal matrix composites were collected [20].

## 2. Materials and Experimentation

*2.1. Base Material.* A 6 mm thick AA7075 plate was chosen as the basis material in this study. The matrix alloy's chemical and mechanical properties are listed in Tables 1 and 2. At a temperature of roughly 180°C, the alloy was artificially aged to achieve the T6 state. Table 3 lists the specifics of the SiC and B<sub>4</sub>C particles utilized as reinforcement in this study. The particles used in this investigation were 35 μm in diameter. By adding 4, 8, 12, and 16wt % of the (SiC + B<sub>4</sub>C) mixture in equal proportions, we were able to create Al-SiC-B<sub>4</sub>C hybrid composites.

*2.2. Composite Fabrication.* The specimen was prepared employing the standard stir-casting method. Figure 1 depicts the experimental setup employed in this study. For the production of each sample, a graphite crucible was used to melt 1000 grams of aluminium in an electric furnace with an argon environment at 8000°C. As a way to improve the matrix alloy's wettability with reinforcements, magnesium (2 wt%) was infused into the molten metal. Magnesium is considered a better wettability agent for SiC. To oxidize the surface of the B<sub>4</sub>C particles, they were baked for 3–4 hours at a temperature of 2000°C in a baking oven. Using a graphite stirrer set to 400 rpm for roughly 10 minutes, this preheated powder was fed into the molten metal at a consistent feed rate using SiC. This ensured a uniform distribution of the powder throughout the metal. A 300 mm long, 80 mm wide, and 40 mm deep injection mold was utilized to pour the liquid combination.

The hybridized composite was allowed to harden at ambient temperature before being taken from the mold and subjected to various mechanical tests. Samples containing 4%, 8%, 12%, and 16% (SiC + B<sub>4</sub>) were prepared using the same procedure.

TABLE 1: Chemical arrangement of AA7075.

Component (wt%)	Magnesium	Silicon	Manganese	Iron	Copper	Zinc	Aluminium
	2.5	0.08	0.04	0.3	1.5	5.6	Remaining

TABLE 2: Mechanical properties of AA7075.

Tensile strength (MPa)	Density ( $\text{g}/\text{cm}^3$ )	Vickers hardness (HV)	% elongation (%)
228	2.81	175	17

TABLE 3: Particulars of SiC and B<sub>4</sub>C particulate.

Reinforcement	Mean particle size ( $\mu\text{m}$ )	Hardness ( $\text{kg}/\text{mm}^2$ )	Density ( $\text{g}/\text{cm}^3$ )	Melting point ( $^{\circ}\text{C}$ )
SiC	35	2,800	3.20	2,700
B <sub>4</sub> C	35	2450	2.52	2,450

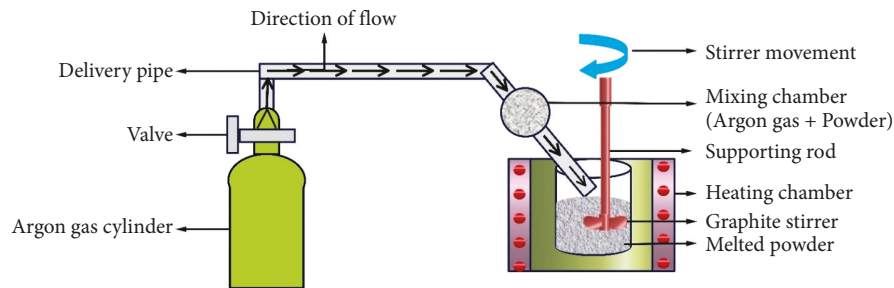


FIGURE 1: Diagram of experimental arrangement.

**2.3. Measurements.** Microstructural investigation was performed by producing cylindrical samples with 6 mm diameters and 20 mm heights. The microstructure samples depicted in Figure 2 were used in the research. An SEM was utilized to examine the microstructure of the Al-SiC-B<sub>4</sub>C mixture. Keller's Reagent (HF/HF/HCl/HNO<sub>3</sub>/H<sub>2</sub>O) and Emery paper (400, 600, and 1000 grades) were utilized to etch samples using Keller's Reagent (H<sub>2</sub>O). Nikon's Eclipse MA-100 optical microscope and JOEL's JSM-6510LV scanning electron microscope were utilized for the microstructure study.

All samples were subjected to a 15-second microhardness test on a Vickers hardness testing method and a force of 1 kg. The hardness of small cuboids was determined using an electric discharge machine. Samples were indented by a diamond indenter, which had square bases and an angle of 136° between them. The Charpy tests, which used specimens 56 × 10 × 10 mm in size, with notch depths of 3 mm, tip radius of 0.30 mm, and angles of 45°, were performed on impact testing machines using these specimens. As shown in Figure 3, the samples used in this study are schematically depicted. All specimens were evaluated three times for hardness and impact strength in order to acquire an average result.

The hybrid composites' tensile behaviour was examined and tested in accordance with the ASTM-E8 standard. Temperatures ranged from 25°C to 30°C and relative humidity ranged from 40 to 60% during the tests on the universal testing equipment. Using the schematic diagram indicated in Figure 4(a), the flat specimens with a thickness

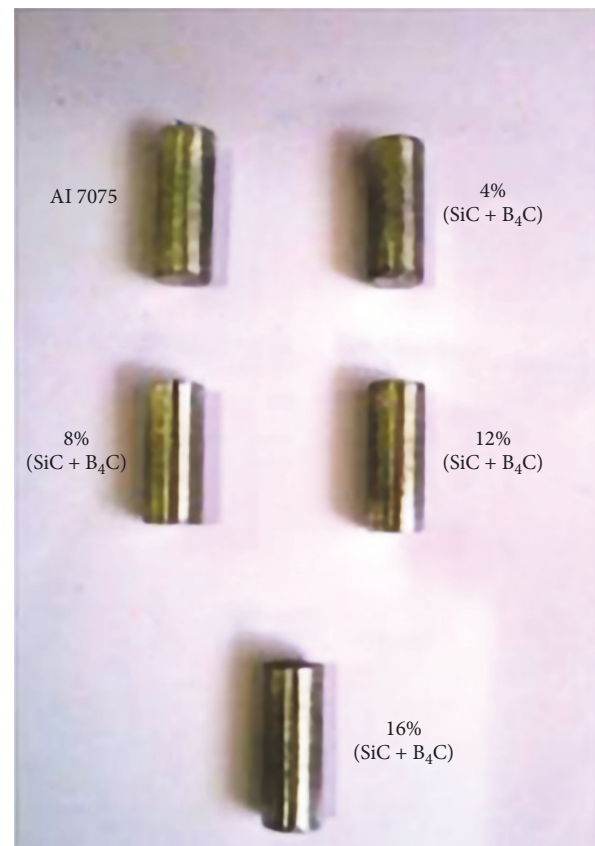


FIGURE 2: Samples for microstructure evaluation.

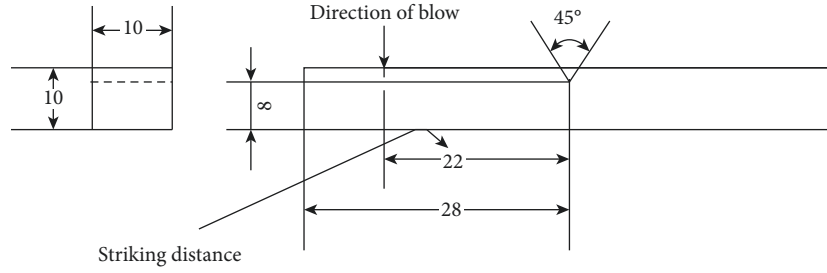


FIGURE 3: Diagram of specimen for impact strength.

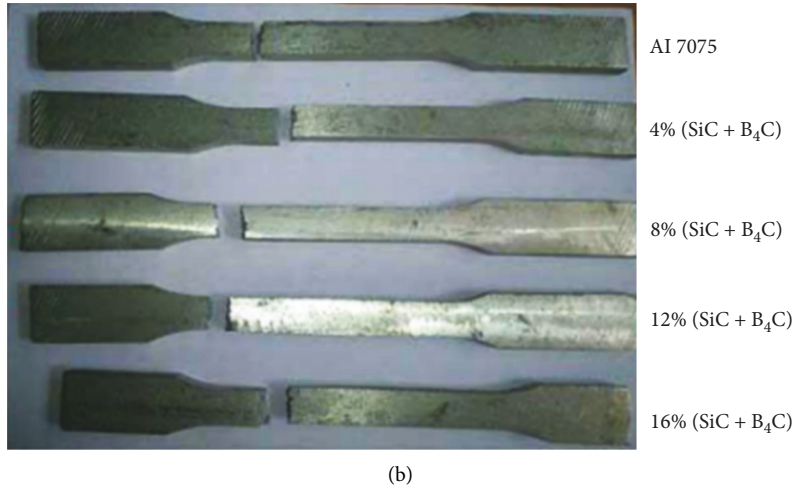
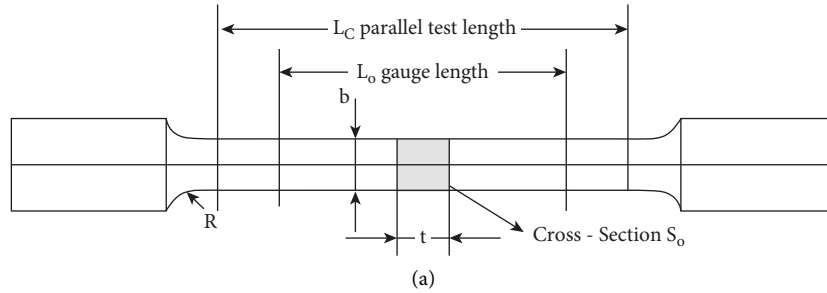


FIGURE 4: Tensile test. (a) Diagram and (b) sample.

of 6 mm were machined to match the dimensions of the schematic diagram. Figure 4(b) shows the tensile test specimens.

The mass and volume of a sample were utilized to calculate the density of the specimen. Equation (1) can be used to determine the density by using the measurements of mass and volume:

$$\text{density} \left( \frac{\text{g}}{\text{cm}^3} \right) = \frac{\text{mass}}{\text{volume}}. \quad (1)$$

The following equation can be used to determine the specimen's porosity using a straightforward relationship:

$$\text{porosity} = 1 - \frac{d}{d_a}, \quad (2)$$

whereas  $d$  is the mass of the specimen and  $d_a$  is the density of the base material.

It will be possible to account for even closed porosity using this straightforward approach.

### 3. Results and Discussion

**3.1. XRD and Microstructural Study.** By using XRD patterns, Figures 5(a)–5(e) depict the matrix alloy and hybridized composites. The prominent peaks in the XRD data belong to aluminium, which is the parent material. Hybrid composites' lower peaks show their SiC and B<sub>4</sub>C content. At the goniometer receiving slit station, the diffractometer uses a graphite curved single crystal monochromator to select CuK radiation ( $\lambda = 1.54\text{\AA}$ ). During the XRD investigation, a diffraction angle ( $2\theta$ ) of 20–1100 was maintained. Figures 5(a)–5(e) depict the occurrence of Si, Al<sub>4</sub>C<sub>3</sub>, and Al<sub>3</sub>BC, all of which were found in the final samples. The hybrid composites' Al<sub>3</sub>BC and Al<sub>4</sub>C<sub>3</sub> maxima, on the other hand, were incredibly low. In an electric furnace, aluminium and boron carbide interacted directly to produce Al<sub>3</sub>BC and Al<sub>4</sub>C<sub>3</sub> [21–23].

Figures 6(a) and 6(b) show scanning electron microscope images of silicon carbide and boron carbide particles,

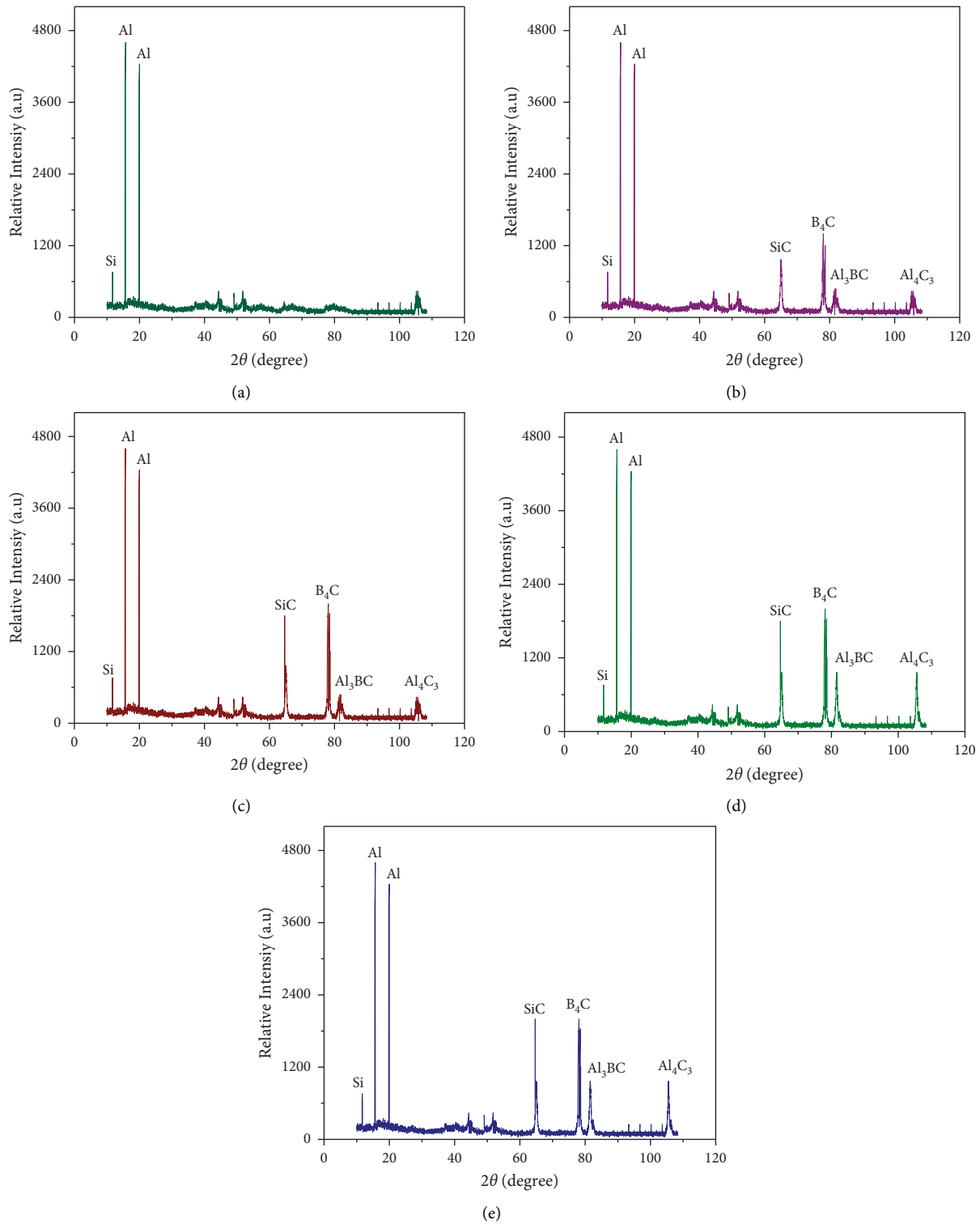


FIGURE 5: X-ray diffraction forms of (a) 0%, (b) 4%, (c) 8%, (d) 12%, and (e) 16% of (silicon carbide + boron carbide) strengthened hybridized composites.

respectively. First-generation Al 7075 grains developing dendritically reveal the interdendritic zone between aluminium and silicon grains in the microstructure of the Al 7075 silicate eutectic. The temperature mismatch between the

molten matrix and the reinforcing particles results in the formation of aluminium. Due to the ceramic particles' weaker heat conductivity compared to Al 7075 melt, the molten matrix is hotter than the temperature of the ceramic particles.

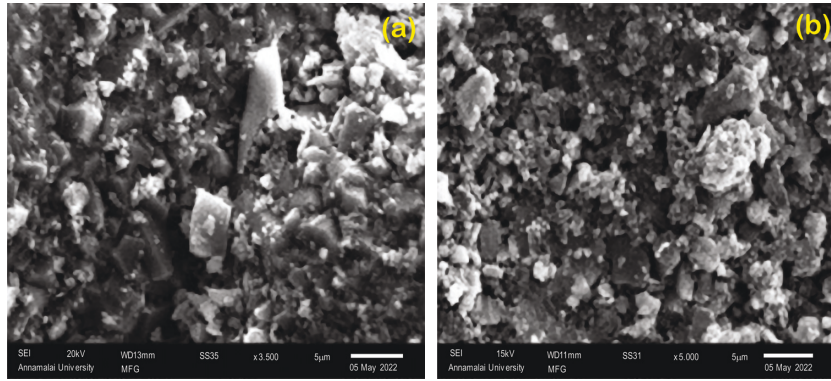


FIGURE 6: (a, b) SEM images of silicon carbide and boron carbide particles.

As a result, the solidification process requires more time to cool hotter particles, which in turn heats the liquid alloy around them. When the hybrid composites were cooled during solidification, they formed dendritic regions. In regions where the dispersion of reinforced particles is not as good, the particle clusters were also detected. No cavities in the interface indicate that the interfacial connection between particles and matrix is strong. According to [20, 24], the reinforcing particulate can prevent dendritic development. Increasing the weight percentage of reinforcement leads to an increased degree of cluster agglomeration as well. In contrast, well-placed agglomerations in the composites can reinforce the composite [25].

**3.2. Impact Strength and Microhardness.** Samples of substrate metal AA7075 and hybridized composites are shown in Table 4. Hybrid composites have higher hardness values than their unreinforced counterparts, and this hardness rises in direct proportion to the weight percentage of reinforcement added. This is in accordance with the investigation that took place previously [26]. The matrix's hardness and resistance to plastic deformation are both improved by the inclusion of hard reinforcing particles [27]. As shown in Figure 7, the hardness increases up to 12%wt fraction, which is shown in the graph. Increasing the density of the particulate mixture within the matrix reduces the hardness of the SiC and B<sub>4</sub>C particles [28]. The ideal hardness of reinforced composites with a (SiC + B<sub>4</sub>C) mixture of 12%wt is 8% greater than the hardness of unreinforced alloys.

Table 5 summarizes the impact test findings for unreinforced alloys and hybrid composites. As shown in Figure 8, as compared to the unreinforced alloy, the impact strength of composites falls as the weight percentage of particles rises in the metal matrix. However, despite the fact that hybrid composites' impact strength tends to decrease, the reduction amount was quite small. One possible explanation for the decrease in strength is the modest change in material properties from ductile to brittle caused by the reinforcement of hard particles [29].

Cracking and decohesion of reinforcing particles lead to the loss of impact strength in composites because of microstructural defects. A reduction in impact strength occurs

as a wt% increase in reinforcement occurs, which leads to a rise in failure rates.

**3.3. Tensile Behavior of Hybrid Composites.** Hybrid composites exhibited a surge in UTS with an increasing weight percentage of the (silicon carbide + boron carbide) mixture in the tensile behavior when the reinforcing mixture was present. Table 6 shows the tensile values as well as the % elongation. Figure 4(b) shows that all samples, even the unreinforced ones, did not break at the center of the gauge length. Because the midsection of a tensile specimen is the weakest when subjected to tensile stresses, it is common for the specimen to shatter. Due to particle concentration, defects, or minute impurities, the center may not be shattered in some cases. For example, the UTS went from 319 MPa at 0% addition to 386 MPa at 12% addition, an increase of 21%. In terms of UTS, the hybrid composite with 12%wt of reinforcement outperforms its 16%wt counterpart. The increased porosity and excessive aggregation of reinforcing particles in the microstructures could be the cause [30]. Porosity in hybrid composites that have been cured reduces material strength, which is caused by the aggregation of tiny particles.

The % elongation of hybrid composites declines as the weight percentage of reinforcement increases in comparison to AA7075. Figure 9 demonstrates how the UTS and elongation percentage change when the wt% of strengthening in the aluminium matrix increases. With the inclusion of strengthening particles and a decrease in the ductility of Al 7075 composition, the percentage elongation decrease may be attributed to these factors.

**3.4. Density and Porosity.** Figures 10 and 11 show the outcome of the measurements of density and porosity. Hybrid composite density decreased after 2.7 g/cm<sup>3</sup> at 0% (silicon carbide + boron carbide) towards 2.61% at 16% (SiC + B<sub>4</sub>C) addition, indicating that the inclusion of reinforcing particles in the metal matrix has little influence on density. There was a recorded 5.2% reduction in density. With the addition of strengthening, the porosity ranges of the strengthened hybridized composites marginally rise. There is an increase in value from 0.35 to 2.14

TABLE 4: Results on microhardness.

Terms of specimen	Hardness1	Hardness2	Hardness 3	Average hardness
AA7075	170	172	168	170
AA7075 + 4% (SiC + B <sub>4</sub> C)	168	169	170	173
AA7075 + 8% (SiC + B <sub>4</sub> C)	171	173	175	173
AA7075 + 12%(SiC + B <sub>4</sub> C)	170	172	173	172
AA7075 + 16% (SiC + B <sub>4</sub> C)	168	173	172	171

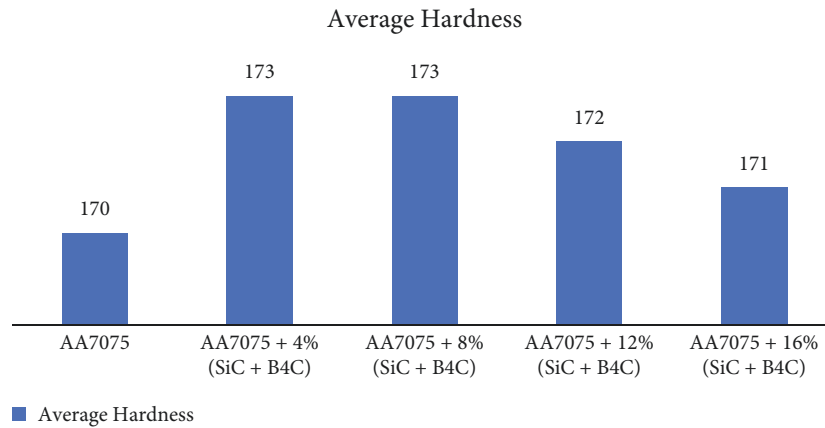


FIGURE 7: Hardness of unreinforced alloy and hybridized composites.

TABLE 5: Impact tests results.

Terms of specimen	Test 1(Nm)	Test 2 (Nm)	Test 3 (Nm)	Mean impact
AA 7075	9.5	9.8	9.5	9.6
AA 7075 + 4% (SiC + B <sub>4</sub> C)	9.4	9.4	9.2	9.33
AA 7075 + 8% (SiC + B <sub>4</sub> C)	8.7	8.75	8.8	8.75
AA 7075 + 12% (SiC + B <sub>4</sub> C)	8.4	8.4	8.2	8.33
AA 7075 + 16% (SiC + B <sub>4</sub> C)	7.9	7.95	7.9	7.92

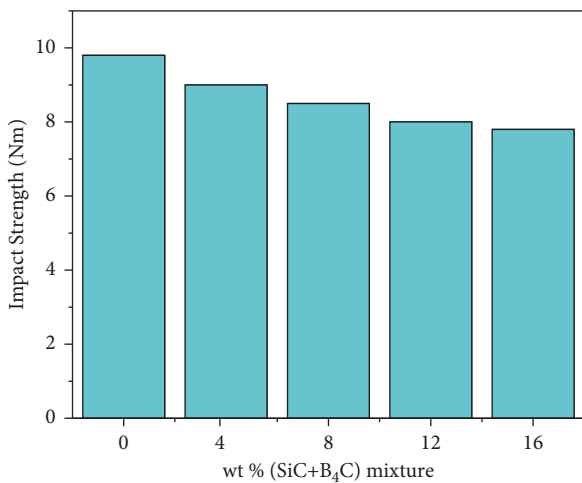


FIGURE 8: Impact strength on variant wt% of (SiC + B<sub>4</sub>C) mixture.

TABLE 6: Results of tensile strength along with % elongation.

Terms of specimen	Ultimate tensile strength (MPa)	% enhancement	% elongation
AA 7075	319	—	8.42
AA 7075 + 4% (SiC + B <sub>4</sub> C)	335	4.8	7.91
AA 7075 + 8% (SiC + B <sub>4</sub> C)	358	12.31	7.32
AA 7075 + 12% (SiC + B <sub>4</sub> C)	386	21.07	6.89
AA 7075 + 16% (SiC + B <sub>4</sub> C)	372	16.7	6.9

when adding 16% (SiC + B<sub>4</sub>C) to the mixture. The authors in [31, 32] found similar results in terms of density and porosity.

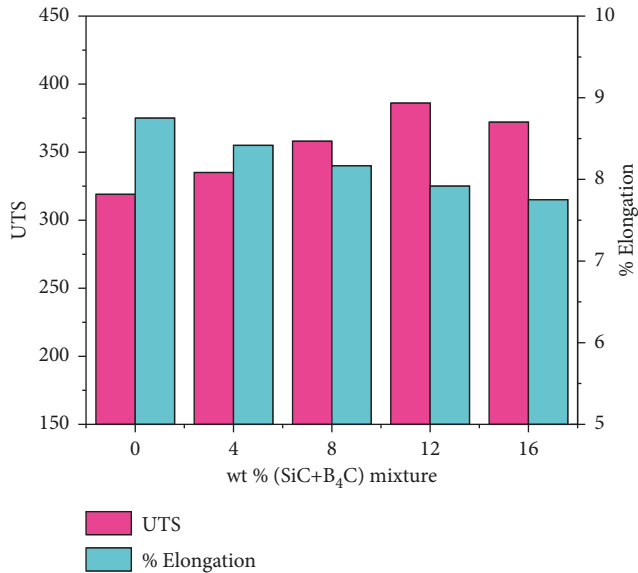


FIGURE 9: Ultimate tensile strength and % elongation for different weight percentages of (SiC + B<sub>4</sub>C) mixture.

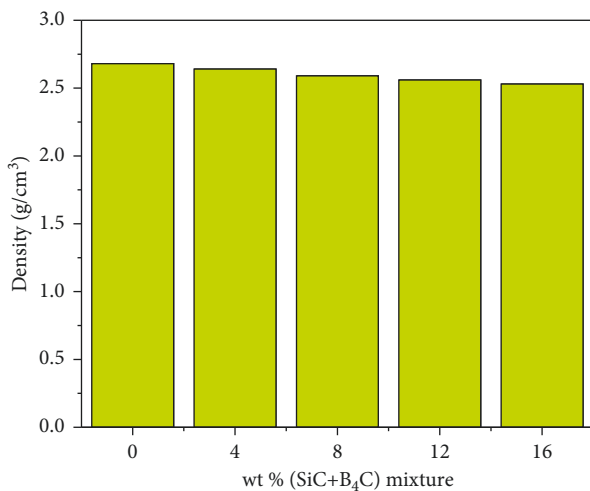


FIGURE 10: Density with variant weight percentage of (SiC + B<sub>4</sub>C) mixture.

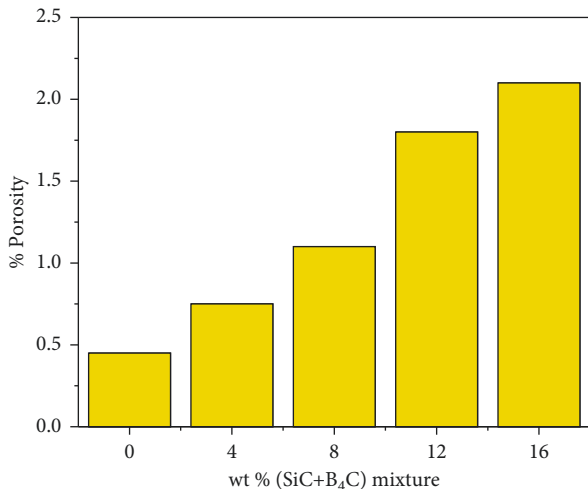


FIGURE 11: Porosity with variant wt% of (SiC + B<sub>4</sub>C) mixture.

## 4. Conclusion

In summary, the stir casting process was employed to create AA7075 reinforced with 4, 8, 12, and 16 weight percentages of (SiC + B<sub>4</sub>C) particulates, and experimental results led to the conclusions listed below:

- (1) The existence of Al 7075, silicon carbide (SiC), aluminum carbide (Al<sub>4</sub>C<sub>3</sub>), ternary alumina-boron carbide (Al<sub>3</sub>BC), boron carbide (B<sub>4</sub>C), and silicon (Si) in the hybridized composites was confirmed by XRD, and SEM micrographs showed good dispersion of the reinforced particles. As the weight percentage of strengthening rises, so does the particle agglomeration.
- (2) It went from 170 HV for an unreinforced alloy to 175 HV for a hybridized component with 12wt% of strengthening in microhardness. An 8% increase in hardness was seen. There was also a minor drop in hardness over 12wt% of reinforcing.
- (3) The impact strength of hybridized composites steadily decreases as reinforcement is added at a marginal rate.
- (4) The ultimate tensile strength of hybrid composites is significantly improved by the addition of reinforcement. When equated to unreinforced alloy, the UTS increases in strength by 21%, from 318 to 386 MPa. With the addition of 16wt% strengthening, however, the hybridized composite's strength decreased slightly.
- (5) With increasing AA matrix composition, the % elongation was identified to be decreased as the strengthening percentage improved.
- (6) A decrease in density and an increase in porosity were noted when reinforcing particulate was added. At 0% SiC + B<sub>4</sub>C adding to 16% Silicon Carbide + Boron Carbide in the metal matrix, the density decreases between 2.7 g/cm<sup>3</sup> and 2.61 g/cm<sup>3</sup>, and the porosity increases between 0.4% and 2.21%.

## Data Availability

No data were used to support this study..

## Conflicts of Interest

The authors declare that they have no conflicts of interest.

## References

- [1] G. Chawla, V. K. Mittal, and S. Mittal, "Experimental investigation of process parameters of al-sic-b4c mmcs finished by a novel magnetic abrasive flow machining setup," *Walailak Journal of Science and Technology*, vol. 18, no. 18, 18 pages, 2021.
- [2] R. Vijayakumar and R. Kirubakaran, "Mechanical behaviour of hybrid metal matrix composite with AL6063/B4C/river sand," *Pakistan Journal of Biotechnology*, vol. 14, pp. 181-184, 2017.
- [3] B. Suresh Babu, "Investigations of the effect of the tool rotational speed on friction stir welded joint on aluminium



- metal matrix hybrid composite. Investigations of the effect of the tool rotational speed on friction stir welded joint on aluminium metal matrix hybrid composite,” *IOP Conference Series: Materials Science and Engineering*, vol. 988, no. 1, Article ID 012045, 2020.
- [4] A. Z. Syahrial and M. A. Pratama, “The influence various boron carbide reinforcement on the microstructure and mechanical properties of ADC12/B4C composite by stir casting,” *AIP Conference Proceedings. The influence various boron carbide reinforcement on the microstructure and mechanical properties of ADC12/B4C composite by stir casting*, vol. 2232, p. 2020, 2020.
  - [5] F. Ahmed, S. Srivastava, and A. B. Agarwal, “Synthesis & Characterization of Al-Ti-Cr MMC as friction material for disc brakes application,” *Materials Today Proceedings*, vol. 4, no. 2, pp. 405–414, 2017.
  - [6] G. S. Matharou and B. K. Bhuyan, “Parametric analysis of electric discharge machining of hybrid composite materials,” *Advances in Engineering Materials*, vol. 7, pp. 329–339, 2021.
  - [7] G. Chawla, V. Kumar, and R. S. Sharma, “Neural simulation of surface generated during magnetic abrasive flow machining of hybrid Al/SiC/B4C-MMCs,” *Journal of Bio- and Tribo-Corrosion*, vol. 7, no. 4, p. 153, 2021.
  - [8] B. Suresh Babu, G. Chandramohan, C. Boopathi, T. Pridhar, and R. Srinivasan, “Production and characterization of mechanical and microstructural behaviour of friction stir welded Al6063 composites reinforced with Gr/B4C/SiC particles,” *Journal of Ceramic Processing Research*, vol. 19, no. 1, pp. 69–74, 2018.
  - [9] Y. S. Bijjargi, V. M. Shinde, A. Mudgal, H. Kumar, and N. E. Prasad, “CFD modeling and optimal design of SiC deposition on the fuel combustion nozzle in a commercial CVD reactor,” *Ceramics International*, vol. 48, no. 8, pp. 11043–11055, 2022.
  - [10] M. Rafiei, M. Salehi, M. Shamanian, and A. Motallebzadeh, “Preparation and oxidation behavior of B4C-Ni and B4C-TiB2-TiC-Ni composite coatings produced by an HVOF process,” *Ceramics International*, vol. 40, no. 8, pp. 13599–13609, 2014.
  - [11] R. Davis, A. Singh, F. L. Amorim, M. J. Jackson, and W. F. Sales, “Effect of tool geometry on the machining characteristics amid SiC powder mixed electric discharge drilling of hybrid metal matrix composite,” *Silicon*, vol. 14, no. 1, pp. 27–45, 2022.
  - [12] B. Varun, V. M. Kumar, L. Jery Rajkumar, and D. R. Medhunhashini, “Characterization of aluminium/(SiC+B4C) ceramic particles reinforced hybrid Surface Composites (SC) fabricated by friction stir processing,” *IOP Conference Series: Materials Science and Engineering*, vol. 932, no. 1, Article ID 012119, 2020.
  - [13] C. T. Guerrero, F. González, T. E. Soto et al., “An overview of the interactions between reinforcements and Al matrices with Si, Cu and Mg as Alloying elements in Aluminum matrix composites: case of oxide reinforcements,” *Materials Research*, vol. 25, 2022.
  - [14] V. K. Lagisetty, A. P. Reddy, and P. V. Krishna, “Dry sliding wear study on aa6061/SiCp nano and aa6061/SiCp/gr hybrid nanocomposites,” *Silicon*, 2022.
  - [15] G. Gobinath and R. Ramachandran, “2nd international conference on sustainable energy resources, materials and technologies,” in *Proceedings of the 2nd International Conference on Sustainable Energy Resources, Materials and Technologies*, vol. 979, ISERMAT, Beijing, China, 2019.
  - [16] O. Meydanoglu, B. Jodoin, and E. S. Kayali, “Microstructure, mechanical properties and corrosion performance of 7075 Al matrix ceramic particle reinforced composite coatings produced by the cold gas dynamic spraying process,” *Surface and Coatings Technology*, vol. 235, pp. 108–116, 2013.
  - [17] T. Senthilvelan, S. Gopalakannan, S. Vishnuvarthan, and K. Keerthivaran, “Fabrication and characterization of SiC, Al<sub>2</sub>O<sub>3</sub> and B4C reinforced Al-Zn-Mg-Cu alloy (AA 7075) metal matrix composites: a study,” *Advanced Materials Research*, vol. 622–623, pp. 1295–1299, 2012.
  - [18] M. C. Jo, J. H. Choi, J. Yoo et al., “Novel dynamic compressive and ballistic properties in 7075-T6 Al-matrix hybrid composite reinforced with SiC and B4C particulates,” *Composites Part B: Engineering*, vol. 174, Article ID 107041, 2019.
  - [19] M. Pul, “Effect of sintering on mechanical property of SiC/B4C reinforced aluminum,” *Materials Research Express*, vol. 6, no. 1, Article ID 016541, 2018.
  - [20] J. P. Ajithkumar and M. Anthony Xavier, “Flank and crater wear analysis during turning of Al 7075 based hybrid composites,” *Materials Research Express*, vol. 6, no. 8, Article ID 086560, 2019.
  - [21] M. Karnam, A. Shivaramakrishna, R. Joshi, T. H. Manjunatha, and K. Veerabhadrapa, “Study of mechanical properties and drilling behavior of Al7075 reinforced with B4C,” *Materials Today Proceedings*, vol. 5, no. 11, pp. 25102–25111, 2018.
  - [22] S. Gopalakannan and T. Senthilvelan, “Synthesis and characterisation of Al 7075 reinforced with SiC and B4C nano particles fabricated by ultrasonic cavitation method,” *Journal of Scientific and Industrial Research*, vol. 74, no. 5, pp. 281–285, 2015.
  - [23] S. Sunil Kumar Reddy, C. Sreedhar, and S. Suresh, “Investigations on Al 7075/nano-SiC/B4C hybrid reinforcements using liquid casting method,” *Materials Today Proceedings*, vol. 46, pp. 8540–8547, 2021.
  - [24] S. K. Tiwari, S. Pal, A. Sharma, A. Dasgotra, and J. K. Pandey, “Investigation of tribological properties of stir cast hybrid aluminum composites,” *Lecture Notes in Mechanical Engineering*, pp. 125–132, 2022.
  - [25] V. C. Uvaraja and N. Natarajan, “Processing of stir cast Al-7075 hybrid metal matrix composites and their characterization,” *International Review of Mechanical Engineering*, vol. 6, no. 4, pp. 724–729, 2012.
  - [26] J. P. Ajithkumar and M. Anthony Xavier, “Cutting force and surface roughness analysis during turning of Al 7075 based hybrid composites,” *Cutting force and surface roughness analysis during turning of Al 7075 based hybrid composites. Procedia Manufacturing*, vol. 30, pp. 180–187, 2019.
  - [27] G. S. Matharou and B. K. Bhuyan, “Hybrid metal matrix composite development by stir casting and environmental concerns,” *Advances in Engineering Materials*, pp. 377–386, 2021.
  - [28] S. Aksöz, S. Kaner, and Y. Kaplan, “Tribological and aging behavior of hybrid Al 7075 composite reinforced with B4C, SiC, and TiB<sub>2</sub>,” *Science of Sintering*, vol. 53, no. 3, pp. 311–321, 2021.
  - [29] S. Thirumalai Kumaran, M. Uthayakumar, and S. Aravindan, “Analysis of dry sliding friction and wear behaviour of AA6351-SiC-B4C composites using grey relational analysis,” *Tribology: Materials, Surfaces & Interfaces*, vol. 8, no. 4, pp. 187–193, 2014.
  - [30] G. Singh and S. Goyal, “Microstructure and mechanical behavior of AA6082-T6/SiC/B4C-based aluminum hybrid composites,” *Particulate Science and Technology*, vol. 36, no. 2, pp. 154–161, 2018.

- [31] D. Bandhu, A. Thakur, R. Purohit, R. K. Verma, and K. Abhishek, "Characterization & evaluation of Al7075 MMCs reinforced with ceramic particulates and influence of age hardening on their tensile behavior," *Journal of Mechanical Science and Technology*, vol. 32, no. 7, pp. 3123–3128, 2018.
- [32] N. Ramadoss, K. Pazhanivel, A. Ganeshkumar, and M. Arivanandhan, "Effect of SiC and MoS<sub>2</sub> Co-reinforcement on enhancing the tribological and anti-corrosive performance of aluminum matrix (Al6063-T6) nanocomposites," *Silicon*, 2021.